https://doi.org/10.1016/j.soildyn.2017.12.023

Energy factors of trilinear SDOF systems representing damage-control buildings with energy dissipation fuses subjected to near-fault earthquakes

Ke Ke[a,b,*], Qingyang Zhao[a,c], Michael C.H. Yam[c], Shuizhou Ke[a]

[a]*College of Civil Engineering, Hunan University, Changsha, China*

[b]*College of Civil Engineering, Tongji University, Shanghai, China*

[c]*Department of Building and Real Estate, The Hong Kong Polytechnic University, Hong Kong, China*

Abstract: This paper presents the energy factor of trilinear single-degree-of-freedom (SDOF) systems representing low-to-medium rise damage-control buildings equipped with energy dissipation fuses under near-fault earthquake ground motions, and the focus is given to the ultimate stage of the systems. The hysteretic behaviour of a damage-control building structure with energy dissipation fuses is firstly idealised by the trilinear kinematic model, and the rationality of the trilinear idealisation is validated by the test result of a representative damage-control structure. Subsequently, the hysteretic law is assigned to SDOF systems and the seismic demand of the systems quantified by the energy factor is examined through extensive nonlinear dynamic analyses with an ensemble of near-fault earthquake ground motions as input excitations. Based on the statistical investigations of more than twenty-one (21) million inelastic spectral analyses of SDOF systems subjected to ground motions, the effect of the post-yielding stiffness ratios and the corresponding inelastic deformation range of the multiple yielding stages on the energy factor of the trilinear SDOF systems are examined in detail, and the corresponding empirical expressions for quantifying the energy factor demand are also developed. The observations of this work show that the energy factor of trilinear SDOF systems subjected to near-fault earthquake ground motions is appreciably influenced by the hysteretic parameters in multiple yielding stages, and engineers have sufficient flexibility to modulate the seismic energy balance of the system by adjusting these influential parameters. The proposed empirical expressions offer a practical tool for estimating the energy factor of a low-to-medium rise damage-control buildings equipped with energy dissipation fuses subjected to near-fault ground motions in the preliminary design phase.

Keywords: energy factor; damage-control; energy dissipation fuse; trilinear systems; near-fault earthquake

---

* Corresponding author.

Email address: keke@hnu.edu.cn (K. Ke)

1. Introduction

In modern seismic engineering, nonlinear response history analysis (NL-RHA) procedure is ~~generally~~ recognised as the most rigorous method to quantify the seismic demand of a structure ~~under~~ subjected to earthquake ground motions. However, from a practical application point of view, ~~practising~~ engineers prefer to utilise static procedures, e.g. direct design methods or nonlinear pushover analysis approaches, to conduct seismic design of a new structure or evaluation of an existing system before using the NL-RHA to finalise the seismic design or the performance assessment of a structure. In this context, a critical issue is the ~~accurate~~ proper quantification of seismic demand indices of structures under earthquake ground motions in static methods, which is also a great challenge in performance-based earthquake engineering.

Research efforts dedicated to quantifying inelastic seismic demands of structures were initiated in the last century. As the foundation of the widely extended forced-based or displacement-based design procedures, indices prescribing the seismic demand in terms of strength [1-5] and deformation [6-9] were explored extensively. For instance, the strength reduction factor [2-4] and the ductility factor [8] that characterise the strength demand and the inelastic deformation demand of an inelastic system, which can also relate the behaviour of the inelastic system with the corresponding elastic system under earthquake ground motions, were found to be reliable indicators in seismic design. Recently, recognising that the seismic performance of a structure can be characterised more reasonably by prescribing both strength demand and displacement demand in seismic design, advanced design procedures with multiple performance indices were developed, ~~i.e.~~ e.g. the performance-spectra-based method proposed by Guo and Christopoulos [10, 11].

In parallel with development of forced-based and displacement-based seismic demand indices and their application in seismic design ~~and evaluation~~ procedures, it has also been recognised that demand indices deduced from the seismic energy balance are promising for quantifying seismic demand of a system subjected to earthquake attacks. The attractiveness of using energy-based demand indices in seismic design has been revealed by studies in recent decades. Among the emerged energy-based demand indices, research findings indicate that an energy factor [12, 13] derived from a modified Housner equation [14] can be used to prescribe the inelastic seismic demand of the system subjected to earthquake ground motions, and both the peak strength demand and the peak deformation demand of ~~a~~ an inelastic system can be considered by the energy factor. In particular, Lee and Goel [12, 13] firstly introduced the energy factor to quantify the seismic demand of elasto-perfectly-plastic (EP) single-degree-of-freedom (SDOF) systems, and empirical expressions of the energy factor for EP SDOF systems were developed using the Newmark and Hall spectra [15] ~~that describe the relationship between the strength factor and the ductility factor~~. Zhai *et al.* [16] studied the influence of near-fault earthquake ground motions on the energy factor of EP SDOF systems and developed a set of design equations for estimating this demand index.

In the meantime, the energy factor was extended to seismic design and evaluation of ductile structures showing the typical EP behaviour. In particular, Goel *et al.* [17] proposed a performance-based-plastic-design (PBPD) methodology with the energy factor of EP SDOF systems quantifying the seismic demand, and the effectiveness of the method ~~have~~ has been examined by applying the procedure in steel moment resisting frames [18], steel frame with buckling restrained braces [19], braced truss moment frames [20, 21] and steel frames with steel plate shear walls [22]. Jiang *et al.* [23] developed an energy-balance-concept-based

multi-mode pushover analysis procedure using the energy factor of EP SDOF systems for prescribing the inelastic seismic demand of structures, and the satisfactory accuracy of the procedure for predicting the peak response demand of ductile steel moment resisting frames showing the typical EP behaviour was also demonstrated by case studies of prototype structures.

More recently, it was observed that the energy factor also serves as a reliable demand index for quantification of peak response demand of an innovative system, i.e. damage-control structures with energy dissipation fuses [24-27]. It is worth pointing out that unlike the aforementioned ductile structures showing the typical EP behaviour, the multi-linear feature is characterised when this novel system is subjected to earthquake attacks, and a typical idealised pushover response of a damage-control structure with energy dissipation fuses is provided in Fig. 1a. When a structure responds in the damage-control (DC) stage with inelastic deformations activated in fuses, the primary system (Fig. 1a) can stay in the elastic state for a wide deformation range and the desirable damage-control behaviour [28] is realised. In this context, the seismic demand can be reasonably estimated by using SDOF systems (Fig. 1b) assigned with a bilinear kinematic hysteretic model with significant post-yielding stiffness ratio [26, 28] ~~which is~~ contributed by the elastic ~~response of the~~ primary system. In cases where the structure responds into the ultimate stage (Fig. 1a) where yielding of the primary system is triggered, SDOF systems with a trilinear hysteretic model with multiple yielding stages should be adopted to ~~characterise~~ describe the nonlinear force-displacement behaviour of the system [28]. Recently, based on the energy factor deduced from the SDOF system with the bilinear kinematic model of significant post-yielding stiffness ratio, the authors [26] proposed a static evaluation procedure for damage-control behaviour

examination of the novel system, and the effectiveness of using the energy factor for predicting the seismic demand of the system responding in the DC stage was validated. However, for a system responds into the ultimate stage where the skeleton pushover response exhibits typical trilinear behaviour, the energy factor derived from the existing EP model or bilinear model with significant post-yielding stiffness ratio may not be adequate for predicting the seismic demand of the system. Thus, recognising that the accurate quantification of seismic demand of damage-control structures in the ultimate stage is also an integral component for developing a full-fledged energy-based design methodology for seismic applications of the novel systems, particularly critical for achieving the life-safety objective under extreme earthquake events, more research efforts are required to fill the knowledge gap.

The present study aims to provide an in-depth understanding of the energy factor of SDOF systems representing low-to-medium rise damage-control building structures equipped with energy dissipation fuses in the ultimate stage under near-fault earthquake ground motions. Essential hysteretic parameters are firstly identified and the hysteretic model validated by an experimental programme is clarified. Then, the energy factor of trilinear SDOF systems representing the damage-control buildings equipped with energy dissipation fuses in the ultimate stage is systematically studied by a parametric study covering a wide spectrum of hysteretic parameters under a large sample of near-fault earthquake ground motions. In total, more than twenty-one million (21,000,000) inelastic spectral analyses of SDOF systems are performed, and the essential parameters that influence the energy factor of the trilinear SDOF systems ~~representing low-to-medium rise damage-control structures with energy dissipation fuses in the ultimate stage~~ are clarified. Empirical expressions based on data regression analyses are also proposed to quantify the energy factor of SDOF systems representing low-

to-medium rise damage-control building structures with energy dissipation fuses in the ultimate stage, which offer a promising tool for practising engineers to conduct a preliminary design of these novel systems entering the ultimate stage.

2. Description and verification of the hysteretic model of the SDOF system

2.1. Hysteretic model and verification

To describe the hysteretic behaviour of a damage-control building structure with energy dissipation fuses responding into the ultimate stage, the trilinear kinematic hysteretic model is adopted and assigned to the representative SDOF systems, and the hysteretic model is schematically illustrated in Fig. 2. In particular, to quantify the multiple yielding stages shown by the structure under lateral loading, the skeleton pushover curve is simplified by a trilinear idealisation and quantified by

$$F = \begin{cases} K\delta & 0 \le \delta \le \delta_{y1} \\ \alpha_1 K\delta + (1-\alpha_1)K\delta_{y1} & \delta_{y1} < \delta \le \delta_{y2} \\ \alpha_2 K\delta + (\alpha_1 - \alpha_2)K\delta_{y2} + (1-\alpha_1)K\delta_{y1} & \delta_{y2} < \delta \end{cases} \quad (1)$$

where K = initial stiffness; δ = displacement; F = force; δ_{y1} = first equivalent yield displacement corresponding to yielding of energy dissipation fuses; δ_{y2} = second equivalent yield displacement corresponding to yielding of the primary system ($\zeta_1\delta_{y1}$); α_1 = post-yielding stiffness ratio of the DC stage and α_2 = post-yielding stiffness ratio of the ultimate stage. Note that α_1 and ζ_1 are the essential parameters for description of the DC stage as well as the damage-control core [26, 28] (Fig. 2) in the hysteretic loops. When the deformation of the structure is restricted in the DC stage, the model is reduced to the bilinear kinematic model with significant post-yielding stiffness ratio.

In the hysteretic model, reference lines are utilised to govern loading and unloading paths,

and critical lines in Fig. 2 describing the hysteretic behaviour are given by

$$F = \alpha_1 K\delta + (1-\alpha_1)K\delta_{y1} \quad \text{for } l_1 \tag{2}$$

$$F = \alpha_1 K\delta - (1-\alpha_1)K\delta_{y1} \quad \text{for } l_2 \tag{3}$$

$$F = \alpha_2 K\delta + (\alpha_1 - \alpha_2)K\delta_{y2} + (1-\alpha_1)K\delta_{y1} \quad \text{for } l_3 \tag{4}$$

$$F = \alpha_2 K\delta + (\alpha_1 - \alpha_2)K(\delta_{y2} - 2\delta_{y1}) + (\alpha_1 - 1)K\delta_{y1} \quad \text{for } l_4 \tag{5}$$

$$F = \alpha_2 K\delta - (\alpha_2 - \alpha_1)K(\delta_{y2} - 2\delta_{y1}) - (\alpha_1 - 1)K\delta_{y1} \quad \text{for } l_5 \tag{6}$$

$$F = \alpha_2 K\delta - (\alpha_1 - \alpha_2)K\delta_{y2} - (1-\alpha_1)K\delta_{y1} \quad \text{for } l_6 \tag{7}$$

$$F = K\delta + K(\delta_{y2} - \delta_{y1}) - \alpha_1 K(\delta_{y2} - \delta_{y1}) \quad \text{for } l_7 \tag{8}$$

$$F = K\delta - K(\delta_{y2} - \delta_{y1}) + \alpha_1 K(\delta_{y2} - \delta_{y1}) \quad \text{for } l_8 \tag{9}$$

Note that in cases where $\alpha_1(\zeta_1\text{-}1)>1$, the yielding of fuses will be triggered during unloading, as shown in Fig. 2a. Otherwise, inelastic actions are activated during loading in the opposite direction, as shown in Fig. 2b. ~~It is noted that~~ l_1, l_2, l_7 and l_8 are used to prescribe the boundary of the damage-control core (DC stage). When the system responds in the damage-control core (Fig. 2), the loading and unloading paths follow the bilinear kinematic law. After the displacement is increased and the system enters the ultimate stage, the damage-control core quantified by l_1 l_2, l_7 and l_8 will translate along l_3, l_4, l_5 and l_6 acting as governing paths. Therefore, the actual hysteretic curve of the system subjected to earthquake ground motions is also dependent on the loading history. Note that cyclic degradation and strength deterioration are not included in the model mentioned above, and hence the hysteretic model is more applicable to damage-control steel systems without evident behaviour deterioration

~~It is worth pointing out that~~ The feasibility of utilising the aforementioned model for characterising the hysteretic behaviour of damage-control building structures with energy dissipation fuses responding into the ultimate stage have been validated by force-displacement

responses from a physical test of a representative system, namely, high strength steel moment resisting frames equipped with sacrificial bays [28]. The concept of the system ~~as a typical damage-control structure with energy dissipation fuses~~ is reproduced in Fig. 3a. In particular, as a typical damage-control ~~structure~~ building, the frame fabricated by high strength steel of a yield strength over 460 MPa was designed as the primary system, and the energy dissipation links in the sacrificial bay were designated as the fuses. To demonstrate the accuracy of the hysteretic model for quantifying the nonlinear force-displacement response of the system, the base shear (F_1) versus first-storey interstorey drift (Δ_1) curves of the specimen responding into the ultimate stage where the primary system developed significant plastic deformation are compared with the trilinear idealisation following the hysteretic law discussed above, and the results are given in Fig. 3c. It can be seen that the result determined by the trilinear model is in good agreement with the nonlinear force-displacement responses of the specimen responding into the ultimate stage in which the primary system developed sufficient yielding, and a pronounced damage-control core can also be extracted from the cyclic response. More information about the test programme and the behaviour of the representative system can be found in [28].

2.2. Energy factor of trilinear SDOF systems representing damage-control structures in the ultimate stage

The governing equation of an inelastic SDOF system representing a low-to-medium rise damage-control building subjected to ground motions is given by

$$m\ddot{\delta} + c\dot{\delta} + F(\delta, \delta_{y1}, \delta_{y2}, \alpha_1, \alpha_2) = -m\ddot{\delta}_g \tag{10}$$

where m = mass of the SDOF system; δ = displacement of the SDOF system; $\dot{\delta}$ = velocity

of the SDOF system; $\ddot{\delta}$ = acceleration of the system; $\ddot{\delta}_g$ = acceleration of an earthquake ground motion; c = damping coefficient and $F(\delta,\delta_{y1},\delta_{y2},\alpha_1,\alpha_2)$ = restoring force of the SDOF system following the trilinear hysteretic law discussed above. Note that for a SDOF system representing a low-to-medium rise damage-control building with energy dissipation fuses responding into the ultimate stage, the restoring force versus displacement relationship follows the trilinear hysteretic law discussed in Section 2.1. Furthermore, utilising the normalisation method proposed by Chopra [29], Eq. (10) can be further normalised and related to a corresponding elastic oscillator assigned with the identical elastic vibration quantities (i.e. mass, period and damping), and given by

$$\ddot{\mu}_s + 2\xi\omega\dot{\mu}_s + \omega^2\bar{F}(\mu_s,1,\zeta_1,\alpha_1,\alpha_2) = -\omega^2\frac{F_e}{F_{y1}}\frac{\ddot{\delta}_g}{S_a} \tag{11}$$

where μ_s = normalised displacement (δ/δ_{y1}) defined as the ductility; $\dot{\mu}_s$ = normalised velocity of the SDOF system ($\dot{\delta}/\delta_{y1}$); $\ddot{\mu}_s$ = normalised acceleration ($\ddot{\delta}/\delta_{y1}$); $\bar{F}(\mu_s,1,\zeta_1,\alpha_1,\alpha_2)$ = normalised restoring force ($F(\delta,\delta_{y1},\delta_{y2},\alpha_1,\alpha_2)/F_{y1}$); ξ = damping ratio; $\omega = \sqrt{\frac{K}{m}}$; F_e = maximum elastic force of the corresponding elastic SDOF system (with the identical mass, period, stiffness, damping as the inelastic SDOF system) under the ground motion; F_{y1} = yield force corresponding to yielding of energy dissipation fuses and S_a = pseudo acceleration coefficient (F_e/m) [29].

Then, relating the skeleton response of the inelastic SDOF system with the trilinear model and the corresponding elastic SDOF system assigned with the identical vibration properties, the energy factor of a SDOF system representing a low-to-medium rise damage-control building responding into the ultimate stage can be determined, which is the ratio of the covered area of the trilinear skeleton pushover response (i.e. the nominal energy of the

system) to the absorbed energy of the corresponding elastic SDOF system (i.e. the covered area of the linear force-displacement response when the system reaches the peak displacement), which is schematically illustrated in Fig. 4.

Thus, the energy factor of a trilinear system [30] is given as follows

$$\gamma = \chi(T;\zeta_1,\mu_s;\alpha_1,\alpha_2,\xi)\boldsymbol{\lambda}_1^{\mathrm{T}}\boldsymbol{\phi}\boldsymbol{\lambda}_2 \tag{12}$$

$$\boldsymbol{\lambda}_1 = \left[1,\ \zeta_1,\ \mu_s - \zeta_1\right]^{\mathrm{T}} \tag{13}$$

$$\boldsymbol{\lambda}_2 = \left[2\mu_s - 1,\ 2\mu_s - \zeta_1,\ \mu_s - \zeta_1\right]^{\mathrm{T}} \tag{14}$$

$$\boldsymbol{\phi} = \mathrm{diag}\left[1, \alpha_1, \alpha_2\right] \tag{15}$$

$$\chi(T;\zeta_1,\mu_s;\alpha_1,\alpha_2,\xi) = \left(\frac{F_{y1}}{F_e}\right)^2 \tag{16}$$

where T= structural period and χ = damage-control factor. Note that the reciprocal term of the square root of the damage-control factor (χ) is also defined as the "strength reduction factor" [2, 3] in extensive works focusing on force-based demand indices. Therefore, the expressions of the energy factor for trilinear SDOF systems, i.e. Eq. (12)-Eq. (16), show that the feature of strength and deformation are both considered when developing the demand index. Also, these equations also indicate that the presence of the damage-control core and the hysteretic parameters in multiple yielding stages (i.e. α_1, α_2, ζ_1, and μ_s) all affect the seismic demand of a damage-control structure equipped with energy dissipation fuses entering the ultimate stage.

3. Ground motion ensemble, parameter matrix, and analysis procedure

In the present study, one hundred (100) acceleration time histories of near-fault earthquake ground motions from various fault types (including strike-slip, reverse, oblique, and normal) and earthquake magnitudes are adopted as input excitations in the parametric study. It is worth pointing out that the ground motions ensemble was developed by Hatzigeorgiou [5, 9]

in works with a focus on strength-based and displacement-based indices. However, during the construction of the ground motion database, the major characteristics of near-fault earthquake ground motions that distinguish them from far-fault ground motions, i.e. intense velocity pulse and displacement pulse of relatively long period, were used to identify a near-fault earthquake ground motion. To produce the ground motions ensemble with generality, the records were downloaded from the ground motion database of PEER [31] considering the earthquakes occurring worldwide. Also, to provide a representative ensemble of strong near-fault earthquake ground motions, the peak ground acceleration of the samples ranges from 0.103 g to 1.298 g, and the records monitored by stations with a distance to fault rupture not larger than 10 km were used. The detailed information including the rationale of the development of the ground motion ensemble and the list of the individual ground motion is documented in [5, 9]. The acceleration spectra of the ground motions with the damping ratio of 5% are given in Fig. 5a, and the displacement spectra are shown in Fig. 5b.

To provide a better understanding of essential parameters influencing the energy factor of the trilinear SDOF systems, particularly under near-fault earthquake ground motions, a parametric study is carried out based on inelastic spectral analyses of SDOF systems with varied hysteretic parameters and the near-fault ground motion ensemble mentioned above. For a typical damage-control building equipped with energy dissipation fuses, recent research findings indicate that a significant post-yielding stiffness ratio of the DC stage (α_1) is more preferable as it may lead to reduced post-earthquake residual deformations [28, 32-34] and uniform plastic energy dissipation [35] in the system. For instance, according to a pilot research work on the seismic response of damage-control structures with energy dissipation fuses in the DC stage, the value of α_1 over 0.75 was recommended ~~based on preliminary~~

~~analyses~~ [35]. Also, it was observed that when the hysteretic model satisfies the first condition in Fig. 2a, i.e. $\alpha_1(\zeta_1\text{-}1)>1$, yielding of fuses during unloading will further mitigate post-earthquake residual deformation and improve the seismic behaviour of the system [28, 31, 32]. Thus, the condition of $\alpha_1(\zeta_1\text{-}1)>1$ is satisfied when constructing the parameter matrix. In the present work, α_1 is increased from 0.5 to 0.9 with an increment of 0.1 (i.e. five values of α_1). On the other hand, after sufficient yielding of the primary system, the post-yielding stiffness ratio generally falls into a narrow spectrum. Thus, this parameter is increased from 0 to 0.05 with an increment of 0.01 (i.e. six values of α_2). In order to investigate the influence of inelastic deformation levels of different yielding stages on the energy factor, ζ_1 ranging from 4 to 8 with an increment of 1 are combined with varied μ_s from 3.5 to 20 with an increment of 0.5. Note that for all combinations of parameters, μ_s is set larger than ζ_1 to produce the parameter matrix with realistic meaning. Note that the damping ratio ranging from 2% to 5% is appropriate for steel structures, and a relatively larger value can be utilised to account for the damping effect of non-structural elements, which is rational for steel systems responding to the limit state. In this context, the damping ratio (ξ) of 5% is assumed in all the analyses, and the corresponding research findings are limited to cases with this damping ratio.

In this work, to directly relate the energy factor with the essential hysteretic parameters quantifying the ultimate stage of a damage-control structure with energy dissipation fuses, a typical constant-ductility-based method [16] is utilised. Specifically, an iterative procedure is adopted to obtain energy factors of trilinear SDOF systems with a prescribed target ductility. A flowchart illustrating the analysis procedure is provided in Fig. 6. Therefore, twenty-one million (21,000,000) inelastic spectral analyses of trilinear SDOF systems are carried out in the parametric study. For the purpose of comparison, the energy factors of EP SDOF systems

(α_1=α_2=0) are also analysed.

4. Analyses results and discussion

Using the ground motions ensemble and the analysis procedure described above, the energy factors of trilinear SDOF systems under various combinations of hysteretic parameters and near-fault earthquake ground motions are obtained. The influences of period (T) and hysteretic parameters including post-yielding stiffness ratios in different yielding stages (α_1 and α_2) as well as the corresponding inelastic deformation levels (ζ_1 and μ_s) on the energy factor are examined. Note that due to the space limit of the paper, only representative results are provided in the following sections when discussing the influences of the essential parameters.

4.1. Effect of post-yielding stiffness ratios

To offer a comprehensive insight into the influence of the post-yielding stiffness ratio in the DC stage (α_1) on the energy factor (γ), representative analysis results in terms of the mean γ demand for trilinear SDOF systems with α_2=0 and various α_1 varied from 0.5 to 0.9 (i.e. α_1=0.5, 0.7 and 0.9) under expected inelastic deformation levels (i.e. ζ_1=4 and 5; μ_s = 6, 8, 10, and 15) are provided in Fig. 7. According to the results given in Fig. 7a, it can be seen that for SDOF systems with a specified μ_s and ζ_1 in the relatively short period region (T<0.3 s), an increasing α_1 results in a pronounced decrease of the mean γ demand. In contrast, the reversed tendency is clear for the mean γ demand in the longer period region (T>0.4 s), as increasing α_1 leads to an evident increase of the mean γ demand, which is indicated by Fig. 7b. It should be noted that Fig. 7 just illustrates the phenomenon that an increasing α_1 results in reversed trend of the γ demand, and the boundary period characterising the reversed trend will also be dependent on the hysteretic parameters. In the current study, it is observed that the boundary

period ranges from 0.3 s to 0.4 s when the hysteretic parameters fall in the analyses spectrum. It is worth pointing out that the similar phenomenon is also characterised if the systems respond in the DC stage, as observed in a previous work [26]. In this context, although increasing the post-yielding stiffness ratio in the DC stage (α_1) is a promising solution for enhancing the seismic performance and mitigating post-earthquake residual deformations of a damage-control structure with energy dissipation fuses, the behaviour of the system in the ultimate stage will also be influenced. Particularly for systems falling in the relatively long period region, special attention should be made for the system responding into the ultimate stage, as the increased α_1 produces higher γ demand. Note that in cases where the value of ζ_1 is significant (indicating that the DC stage has a wide deformation range), the increase of the mean γ demand induced by a significant α_1 in the long period region is more substantial, showing the cascading effect between α_1 and ζ_1 on the γ demand, which are the key parameters of the damage-control core in the DC stage. For example, for systems with ζ_1=5 and μ_s=8 in the relatively long period region as shown in Fig. 7b, the increase of the mean γ demand for the system with T=1 s is over 70% when α_1 is increased from 0 to 0.7. Comparatively, for the SDOF counterparts with ζ_1=4 and μ_s=8 given in Fig. 7b, the corresponding increase of the mean γ demand for the system with T=1 s is around 50% with α_1 increasing from 0 to 0.7. To further clarify the effect of α_1 on the γ demand, all the analysis results of the mean γ demand with ζ_1=4 as representation are illustrated in Fig. 8. In particular, all data points with α_1=0.5 are compared with the counterparts with α_1>0.5. As can be seen, for the representative systems in the specified short period region (0.1 s<T<0.3 s), the data points are clustered below the forty-five degree line, and indicate that the mean γ demand consistently decreases with α_1 increasing, whereas the reversed trend can be observed for the

systems in the longer period region.

To illustrate the effect of the post-yielding stiffness ratio of the ultimate stage (α_2) on the γ demand, representative mean γ demand spectra for the trilinear SDOF systems with α_1=0.5 and varied values of α_2 are given in Fig. 9. Also, representative results with α_2>0, i.e. α_2=0.02 and α_2=0.05, are plotted against the counterparts with α_2=0, as illustrated in Fig. 10. According to these results, it can be seen that as α_2 is varied in a relatively narrow range, the influence of α_2 on the γ demand is not as appreciable as α_1, which is shown by the representative results provided in Fig. 9 and Fig. 10. In particular, the increasing of α_2 results in very slight decreasing of the mean γ demand for both short-period and long period-region, although such trend becomes more evident when the system is expected to experience significant inelastic deformations in the ultimate stage. For instance, for the trilinear SDOF system with ζ_1=4 and μ_s =15, there is only 7% reduction of γ in average for the SDOF system of 0.1 s when α_2 is increased from 0.02 to 0.05. In general, the change of α_2 does not result in an evident fluctuation of mean γ demand for the trilinear SDOF systems falling in the spectrum of the parameter matrix, indicating that the dependency of γ on α_2 is relatively small.

In the meantime, to characterise the influence of the post-yielding stiffness ratios on the degree of dispersion of the mean γ demand of the trilinear SDOF systems subjected to the near-fault ground motion ensemble, the coefficient of variation (COV) of γ, i.e. the standard deviation to the mean ratio of γ, is extracted from the analysis result database. The COV spectra of the representative mean γ spectra are shown in Fig. 11. As can be seen from Fig. 11a, there is generally an evident decrease of COV of the mean γ demand with α_1 increasing, irrespective of the other hysteretic parameters, i.e. α_2, ζ_1 and μ_s. Taking the SDOF systems with ζ_1=4 and μ_s=8 as an example, it is observed that the COVs of the mean γ demand for EP

SDOF systems approach unity, whereas the counterparts for the trilinear SDOF systems with α_1 =0.9 as the extreme case are below 0.5. From the perspective of seismic behaviour of the systems, this trend indicates that maintaining significant post-yielding stiffness ratio in the DC stage also enhances the performances of the system in the ultimate stage, since more stable seismic responses with reduced dispersion can be obtained. Also, Fig. 11a indicates that the dependency of the dispersion of γ on the structural period is influenced by the level of α_1. Specifically, the COV of the mean γ demand is less dependent on the period when α_1 is significant, but the dependency of the COV of the mean γ demand for systems with a smaller α_1 becomes relatively erratic. In contrast, Fig. 11b shows that α_2 has an insignificant effect on the dispersion of γ, as there is not a wild fluctuation of the mean γ spectra when α_2 is varied in the analysed range.

4.2. Effect of inelastic deformation levels

On the other hand, by comparing the results with different combinations of inelastic deformation levels presented in Fig. 7 and Fig. 9, the effect of ζ_1 and μ_s on the mean γ demand can also be observed. In particular, for the trilinear SDOF systems in the short period region, the increasing μ_s produces an evident increase of the mean γ demand, and the phenomenon of the "energy lock" is seen, indicating that the seismic energy balance is hard to achieve for short-period systems entering the inelastic range. It is worth pointing out that this phenomenon is also observed from the distribution of the mean γ demand of EP SDOF systems (α_1=α_2=0) shown in the figures. In particular, for short-period SDOF systems with a ductility factor prescribing the inelastic deformation levels, the mean γ demand is much larger than unity, indicating that the yielding behaviour of a SDOF system produces a very high seismic demand. However, as discussed in the previous section and shown in Fig. 7,

enhancement of the post-yielding stiffness ratio in the DC stage, i.e. α_1, leads to decrease in the γ demand for short-period systems, which provides a potential solution to overcoming the "energy lock". In contrast, for the trilinear SDOF systems in the long period region, the mean γ demand decreases with increase of μ_s, and this observation is understandable since the seismic energy balance of a long-period system is generally achieved by developing inelastic deformations, and the covered area of the skeleton pushover response curve can be much smaller than that of the corresponding elastic SDOF systems, as indicated by the decreasing of the mean γ demand. It should also be noted that for systems with a prescribed μ_s, an increasing ζ_1 (a wider deformation range in the DC stage) results in reduction of the mean γ demand in the short-period region, but the increase of the mean γ demand can be observed for systems with longer period (Comparing the case of ζ_1=4, μ_s =8 with the counterpart with ζ_1=5, μ_s =8 in Fig. 7). Thus, the influence of damage-control core on the mean γ demand of the trilinear SDOF systems is characterised again.

Likewise, the COV spectra of representative mean γ provided in Fig. 11 also illustrates the influence of inelastic deformation levels on the dispersion of the mean γ demand. As expected, the increase of μ_s results in increase of the COV of γ over the analysed period range included in the parametric study. In contrast, for the cases with the identical μ_s, an increasing ζ_1 may result in the reversed trend (Comparing the case of ζ_1=4, μ_s =8 with ζ_1=5, μ_s =8 in Fig. 11a), particularly in cases with a significant α_1, which is owing to the presence of the damage-control core again.

5. Empirical expressions of the energy factor

5.1. Empirical expression of the energy factor of trilinear SDOF systems

From a practical application point of view and the performance-based seismic engineering,

although the damage-control structures are expected to stay in the DC stage to realise the desirable damage-control behaviour under earthquakes in the design-level, the behaviour of the system responding into the ultimate stage should also be included the seismic design procedure to rationally exploit the inelastic deformation capacity of the primary system under extreme earthquake events. Therefore, the appropriate quantification of the seismic demand of the systems in the ultimate stage is also essential. In this regard, it is desirable to relate the nonlinear vibration properties and the nonlinear hysteretic parameters with the energy factor (γ) of the trilinear SDOF systems representing the damage-control structures with energy dissipation fuses responding into the ultimate stage. In this study, based on the analysis database in the parametric study, a two-step nonlinear regression procedure is conducted and a preliminary design model is developed. Specifically, the relationship between the mean energy factor (γ) and the influential parameters including structural period (T), inelastic deformation range of the DC stage (ζ_1), and the target ductility (μ_s) is regressed firstly. Then, the influence of the post-yielding stiffness ratios (i.e. α_1 in the DC stage and α_2 in the ultimate stage) is also employed in the regression model. In this procedure, the Table Curve 3D is utilised to seek for the optimum empirical expressions, and the following equation is developed.

$$\gamma = \frac{\boldsymbol{\lambda}_1^{\mathrm{T}} \boldsymbol{\phi} \boldsymbol{\lambda}_2}{\left(\dfrac{1}{a + bT + c\ln T + d\mathrm{e}^{-T} + \dfrac{f}{\mu_s - 1}} + 1\right)^2} \tag{17}$$

In Eq. (17), a, b, c, d, and f are regressed coefficients accounting for the influence of post-yielding stiffness ratios in different yielding stages, i.e. α_1 for the DC stage as well as α_2 for the ultimate stage, and inelastic deformation levels in various yielding stages, i.e. ζ_1 and μ_s. e is the natural constant (Euler's number). Note that the proposed equation is one of the

simplest equations after a trial-and-error procedure based on 40000 mathematical expressions (e.g. polynomials, nonlinear exponential functions, power functions), and the regressed coefficients are determined based on the least square ~~principal~~ principle.

In the second step, to account for the influence of post-yielding stiffness ratios (α_1 and α_2) and the potential interaction between them on the distribution of the mean γ demand, the regressed coefficients with a provided ζ_1 are given by the following equations based on nonlinear regression analyses.

$$a(\alpha_1,\alpha_2)=a_1+a_2\alpha_1+a_3\alpha_2+a_4\alpha_1^2+a_5\alpha_2^2+a_6\alpha_1\alpha_2 \tag{18}$$

$$b(\alpha_1,\alpha_2)=b_1+b_2\alpha_1+b_3\alpha_2+b_4\alpha_1^2+b_5\alpha_2^2+b_6\alpha_1\alpha_2 \tag{19}$$

$$c(\alpha_1,\alpha_2)=c_1+c_2\alpha_1+c_3\alpha_2+c_4\alpha_1^2+c_5\alpha_2^2+c_6\alpha_1\alpha_2 \tag{20}$$

$$d(\alpha_1,\alpha_2)=d_1+d_2\alpha_1+d_3\alpha_2+d_4\alpha_1^2+d_5\alpha_2^2+d_6\alpha_1\alpha_2 \tag{21}$$

$$f(\alpha_1,\alpha_2)=f_1+f_2\alpha_1+f_3\alpha_2+f_4\alpha_1^2+f_5\alpha_2^2+f_6\alpha_1\alpha_2 \tag{22}$$

The regressed coefficients a_i, b_i, c_i, d_i, and f_i for various values of ζ_1 are provided in Table 1 along with the coefficient of determination (R^2). Note that the developed empirical expression in Eq. (17) for the energy factor also follows the boundary condition given by:

$$\gamma(T,\zeta_1,\mu_s)=1 \quad (\zeta_1,\mu_s \to 1) \tag{23}$$

This boundary condition is based on the definition of the energy factor as well as the classical Housner's equation [14], and the constant value of unity is obtained when a system responds in the elastic range.

It is also worth pointing out that according to the definition of the energy factor discussed above, the damage-control factor can also be reduced to the widely used strength reduction factor, and thus the proposed equation also satisfies an inherent condition, which is given by

$$\chi(\zeta_1,\mu_s;\alpha_1,\alpha_2)=1 \quad (T \to 0) \tag{24}$$

This equation indicates that very stiff systems should be designed as elastic systems, echoing the phenomenon of the "energy lock" as observed in the parametric analysis.

5.2. Validation of the proposed empirical expressions

To validate the effectiveness of the proposed model for quantifying the energy factor of the trilinear SDOF systems representing low-to-medium rise damage-control buildings responding into the ultimate stage, the energy factor (γ) spectra computed by the proposed equations (Eq. (17)-Eq. (22)) are compared with the counterparts obtained from inelastic spectral analyses, and representative results are provided in Fig. 12. To characterise a direct comprehension of the difference between the mean γ demand of trilinear SDOF systems representing low-to-medium rise damage-control buildings responding into the ultimate stage and the classical EP SDOF system, γ determined from the Newmark and Hall inelastic spectra [15], which are utilised to quantify the energy factor of EP SDOF systems and extended to energy-based design of conventional ductile structures, are applied to compute the energy factor of the SDOF systems. More specifically, the energy factor of an EP SDOF system can be obtained by substituting $\alpha_1=\alpha_2=0$ into Eq. (12)-(16) and is reduced to

$$\gamma = \chi(2\mu_s - 1) \tag{25}$$

Note that in this case, the reciprocal of damage-control factor (χ) is the square of the strength reduction factor of an EP SDOF system, and the design spectra proposed by Newmark and Hall [15] can be substituted into Eq. (25) for quantifying the energy factor. Hence, the χ spectra for EP SDOF systems are given as follows:

$$\chi = \begin{cases} 1 & 0 \le T < \dfrac{T_1}{10} \\ \dfrac{1}{[\sqrt{2\mu_s - 1}\ (\dfrac{T_1}{4T})^{2.513^{\log(\frac{1}{\sqrt{2\mu_s-1}})}}]^2} & \dfrac{T_1}{10} \le T < \dfrac{T_1}{4} \\ \dfrac{1}{2\mu_s - 1} & \dfrac{T_1}{4} \le T < T_1' \\ (\dfrac{T_1}{T\mu_s})^2 & T_1' \le T < T_1 \\ \dfrac{1}{\mu_s^{\,2}} & T_1' \le T \end{cases} \tag{26}$$

In Eq. (26), T_1=0.57 s and $T_1' = T_1\ (\sqrt{2\mu_s - 1} / \mu_s)$. Note that the expressions are also based on the assumed damping ratio of 5%. The results illustrated in Fig. 12 indicate that the proposed expressions in the present study can result in satisfactory estimates of the mean γ demand of trilinear SDOF systems with varied post-yielding stiffness ratios and inelastic deformation levels. In contrast, the energy factor spectra derived from the Newmark and Hall inelastic spectra generally produce inconsistent results of the mean γ, and non-conservative estimates are obtained for systems falling in the long-period region (T>0.3 s). Particularly for systems that are expected to experience significant inelastic deformations in the ultimate stage, the inconsistency between the energy factor spectra applicable to EP SDOF systems and the counterparts of trilinear SDOF systems with multiple yielding stages becomes more pronounced.

To further demonstrate the ability of the proposed model for quantifying the mean γ demand of trilinear SDOF systems with the presence of a damage-control core, all data points for representative cases with ζ_1=4 and ζ_1=5 determined by inelastic spectral analyses are plotted against the counterparts computed by the developed empirical expressions, and the comparison is presented in Fig. 13. As can be seen in the figure, the data points are clustered

close to the forty-five degree diagonal line, indicating that the developed empirical expressions have satisfactory accuracy for predicting the mean γ demand of the trilinear SDOF systems. Especially for the oscillators in the relatively long-period region (T>0.4 s) which may be used to represent building structures in practical engineering, the discrepancies are generally within 10%, and practising engineers can utilise the proposed empirical expressions to conduct a preliminary design conveniently.

5.3. Comments and design considerations

Based on the observations mentioned above and the effects of the influential hysteretic parameters on the energy factor (γ) of the trilinear SDOF systems representing low-to-medium rise damage-control buildings with energy dissipation fuses responding to the ultimate stage, the desirable features of the novel systems subjected to near-fault earthquake ground motions are also revealed: (1) The trilinear force-displacement response of a damage-control structure with energy dissipation fuses enables modulation of the seismic energy balance of the structure subjected to the earthquake ground motions, as the γ demand quantifying the seismic demand of the system is influenced by multiple parameters. In particular, compared with the conventional ductile structures that can be represented by an EP SDOF system or a bilinear counterpart with negligible post-yielding stiffness ratio, the hysteretic parameters (i.e. multiple post-yielding stiffness ratios and inelastic deformation levels) of the trilinear SDOF systems all influence the seismic energy balance of the system, and thus a designer could explicitly design the seismic energy balance of a damage-control system equipped with energy dissipation fuses by adjusting the influential parameters with sufficient flexibility. (2) For a damage-control structure with energy dissipation fuses responding into the ultimate stage, the presence of the damage-control core with a significant

post-yielding stiffness ratio (α_1) results in more controllable seismic behaviour with decrease in dispersion of the seismic response, and hence the uncertainty induced by interaction between nonlinearity of the structural force-displacement response and ground motion properties can be reduced. In this context, the response of the ~~damage-control structure equipped with energy dissipation fuses~~ system under the expected near-fault earthquakes can be quantified with enhanced accuracy.

It is worth pointing out that in practical engineering, designers can develop a damage-control ~~structure~~ building achieving the optimised performance in the ultimate stage by modulating the structural arrangement, and thus the optimised hysteretic parameters can be realised. For instance, for a multi-storey building structure in the long period region which is expected to experience the near-fault earthquake ground motions, to eliminate the detrimental effect produced by increasing of the γ demand induced by significant post-yielding stiffness ratio (α_1) in the DC stage, a relatively wide inelastic deformation range in the ultimate stage (i.e larger μ_s) can be prescribed. However, it should be noted that the realisation of the target hysteretic parameters is still dependent on specific structural arrangement, and the proposed preliminary designed model in this paper just puts forth a tool ~~for an engineer~~ to determine the term of the demand of the structure responding into the ultimate stage. Also, since this work is based on the SDOF analogy, the findings from this research are limited to low-to-medium rise buildings dominated by the fundamental vibration mode. For taller structures, the quantification of the seismic demand should employ multi-modes and the interactive effect among them.

6. Conclusions

This paper presents the energy factor spectra of trilinear single-degree-of-freedom (SDOF)

systems representing low-to-medium rise damage-control buildings equipped with energy dissipation fuses under near-fault earthquake ground motions, and the focus is given to the ultimate stage of the systems. The main innovation of this research is the quantification of the influence of the essential hysteretic parameters on the energy factor when the systems are subjected to near-fault earthquake ground motions, and the effect of the post-yielding stiffness ratios and the inelastic deformation levels in different yielding stages ~~on the distribution of the energy factor~~ are carefully examined and discussed based on more than twenty-one (21,000,000) million inelastic spectral analyses of SDOF systems. The comprehensive investigation of the essential parameters influencing the energy factor of the trilinear SDOF systems ~~representing low-to-medium rise damage-control buildings responding into the ultimate stage~~ can lead to the following observations:

1. For a trilinear SDOF system with the presence of a damage-control core under the near-fault earthquake ground motions, the increase of post-yielding stiffness ratio in the damage-control (DC) stage (α_1) leads to a pronounced decrease of the energy factor (γ) in average for relatively short-period systems ~~(T<0.3 s)~~, but the reversed trend is observed for the systems with longer period. According to the coefficient of variation (COV) spectra of the statistical results, an increasing ~~of~~ α_1 results in a general decrease of the dispersion of the γ demand over the analysed period region. These features are more evident in cases where the system has a wider deformation range in the DC stage, i.e. a larger ζ_1, whereas is less pronounced when the ductility (μ_s) is substantial. In contrast, as the post-yielding stiffness ratio in the ultimate stage (α_2) generally falls in a narrow range, observations from the statistical investigation indicate that the influence of this parameter on the energy factor of trilinear SDOF systems and the corresponding

dispersion is insignificant.

2. The increase of μ_s results in an increase of the mean γ demand for short-period systems, whereas the mean γ demand is decreased with μ_s increasing for systems in the longer period region. As for the dispersion of the data, the ~~coefficient of variation (~~COV~~)~~ spectra of the mean γ demand show that the increase of μ_s leads to more evident scatteration of the γ demand, irrespective of other hysteretic parameters. Comparatively, for short-period systems with a prescribed μ_s, the mean γ demand tends to decrease with ζ_1 increasing, whereas the reversed trend can be observed for the systems with a longer period, and this phenomenon is also contributed by the presence of the damage-control core with a significant α_1. Likewise, for all the systems with the identical μ_s, the COV spectra of the mean γ demand indicate that enlarging the deformation range of the DC stage, i.e. the value of ζ_1, is effective for producing the γ demand with reduced dispersion owing to the contribution of significant α_1 of the damage-control core.
3. The multiple yielding stages of the trilinear SDOF systems and the presence of the damage-control core provide sufficient flexibility for modulation of the seismic energy balance of the damage-control structures equipped with energy dissipation fuses, and the interdependence of the strength and deformation demand which can be observed in conventional EP SDOF systems is decoupled.
4. Empirical expressions of the mean γ demand for SDOF systems subjected to near-fault earthquake ground motions are developed ~~in this paper~~ based on the database of the inelastic spectral analyses of SDOF systems with various hysteretic parameters, and practising engineers can adopt the proposed expressions to quantify the γ demand in the preliminary design phase.

Currently, research works on using energy factors of equivalent trilinear SDOF systems for quantifying the seismic demand of taller damage-control structures equipped with energy dissipation fuses are being conducted.

Acknowledgments

This research is financially supported by the Fundamental Research Funds for the Central Universities of China (No. 531107050968) and the National Science Foundation of China (Grant No. 51708197).

References

[1] EC8. Design of structures for earthquake resistance, Part 1: General rules, seismic actions and rules for buildings, European Standard EN 1998-1:2004. European Committee for Standardization (CEN), Brussels, 2008.

[2] Uang CM. Establishing R (or Rw) and Cd Factors for Building Seismic Provisions. J Struct Eng 1991; 117(1): 19-28.

[3] Miranda E. Site-dependent strength reduction factors. J Struct Eng ASCE 1993; 119(12): 3503-3519.

[4] Jalali RS, Trifunac MD. A note on strength-reduction factors for design of structures near earthquake faults. Soil Dyn Earthq Eng 2008; 28(3):212-222.

[5] Hatzigeorgiou GD. Behavior factors for nonlinear structures subjected to multiple near-fault earthquakes. Comput Struct 2010; 88(5): 309-321.

[6] Chopra AK, Chintanapakdee C. Inelastic deformation ratios for design and evaluation of structures: Single-degree-of-freedom bilinear systems. J Struct Eng ASCE 2004; 130(9):

1309-1319.

[7] Hatzigeorgiou GD, Beskos DE. Inelastic displacement ratios for SDOF structures subjected to repeated earthquakes. Eng Struct 2009; 31(11): 2744-2755.

[8] Hatzigeorgiou GD. Ductility demand spectra for multiple near- and far-fault earthquakes. Soil Dyn Earthq Eng 2010; 30(4): 170-183.

[9] Hatzigeorgiou GD, Papagiannopoulos GA, Beskos DE. Evaluation of maximum seismic displacements of SDOF systems from their residual deformation. Eng Struct 2011; 33(12): 3422-3431.

[10] Guo JWW, Christopoulos C. Performance spectra based method for the seismic design of structures equipped with passive supplemental damping systems. Earthq Eng Struc Dyn 2013; 42(6): 935-952.

[11] Guo JWW, Christopoulos C. A procedure for generating performance spectra for structures equipped with passive supplemental dampers. Earthq Eng Struc Dyn 2013; 42(9): 1321-1338.

[12] Lee SS, Goel SC, Chao SH. Performance-based design of steel moment frames using a target drift and yield mechanism. Research Report No. UMCEE 01-17, Dept. of Civil and Envr. Engr., Univ. of Michigan, Ann Arbor, MI. 2001.

[13] Leelataviwat S, Saewon W, Goel SC. Application of energy balance concept in seismic evaluation of structures. J Struct Eng 2009; 135(2): 113-121.

[14] Housner GW. Limit design of structures to resist earthquakes. In: Proceedings of the first world conference on earthquake engineering. 1959.

[15] Newmark NM, Hall WJ. Earthquake spectra and design, monograph. Oakland (CA): Earthquake Engineering Research Institute (EERI). 1982.

[16] Zhai C, Ji D, Wen W, Lei W, Xie L. Constant ductility energy factors for the near-fault pulse-like ground motions. J Earthq Eng 2016; 1-16.

[17] Goel SC, Liao WC, Bayat MR, Chao SH. Performance-based plastic design (PBPD) method for earthquake-resistant structures: an overview. Struct Des Tall Spec 2010; 19(1-2): 115-137.

[18] Banihashemi MR, Mirzagoltabar AR, Tavakoli HR. Development of the performance based plastic design for steel moment resistant frame. Int J Steel Struct 2015; 15(1): 51-62.

[19] Sahoo DR, Chao S. Performance-based plastic design method for buckling-restrained braced frames. Eng Struct 2010; 32(9): 2950-2958.

[20] Wongpakdee N, Leelataviwat S, Goel SC, Liao WC. Performance-based design and collapse evaluation of buckling restrained knee braced truss moment frames. Eng Struct 2014; 60: 23-31.

[21] Heidari A, Gharehbaghi S. Seismic performance improvement of special truss moment frames using damage and energy concepts. Earthq Eng Struct Dyn 2015; 44(7): 1055-1073.

[22] Kharmale SB, Ghosh S. Performance-based plastic design of steel plate shear walls. J Constr Steel Res 2013; 90: 85-97.

[23] Jiang Y, Li G, Yang D. A modified approach of energy balance concept based multimode pushover analysis to estimate seismic demands for buildings. Eng Struct 2010; 32(5): 1272-1283.

[24] Vargas R, Bruneau M. Analytical Response and Design of Buildings with Metallic Structural Fuses. I. J Struct Eng 2009; 135(4): 386-393.

[25] Vargas R, Bruneau M. Experimental response of buildings designed with metallic structural fuses. II. J Struct Eng 2009; 135(4): 394-403.

[26] Ke K, Yam MCH, Ke S. A dual-energy-demand-indices-based evaluation procedure of damage-control frame structures with energy dissipation fuses. Soil Dyn Earthq Eng 2017; 95: 61-82.

[27] Connor JJ, Wada A, Iwata M, Huang YH. Damage-controlled structures .1. Preliminary design methodology for seismically active regions. J Struct Eng 1997; 123(4): 423-431.

[28] Ke K, Chen YY. Seismic performance of MRFs with high strength steel main frames and EDBs. J Constr Steel Res 2016; 126: 214-228.

[29] Chopra AK. Dynamics of structures: theory and applications to earthquake engineering (2nd ed.). Prentice-Hall, Upper Saddle River, NJ. 2001.

[30] Ke K, Ke S, Chuan G. The energy factor of systems considering multiple yielding stages during ground motions. Soil Dyn Earthq Eng 2015; 71: 42-48.

[31] Pacific Earthquake Engineering Research Center. PEER strong motion database. <http://peer.berkeley.edu/smcat>

[32] Kawashima K, Macrae GA, Hoshikuma J, Nagaya K. Residual displacement response spectrum. J Struct Eng 1998; 124(5): 523-530.

[33] Macrae GA, Kawashima K. Post-earthquake residual displacements of bilinear oscillators. Earthquake Eng Struc Dyn 1997; 26(7): 701-716.

[34] Pettinga D, Christopoulos C, Parnpanin S, Priestley N. Effectiveness of simple approaches in mitigating residual deformations in buildings. Earthq Eng Struct Dyn 2007; 36(12): 1763-1783.

[35] Nakashima M, Saburi K, Tsuji B. Energy input and dissipation behaviour of structures with hysteretic dampers. Earthq Eng Struct Dyn 1996; 25(5): 483-496.

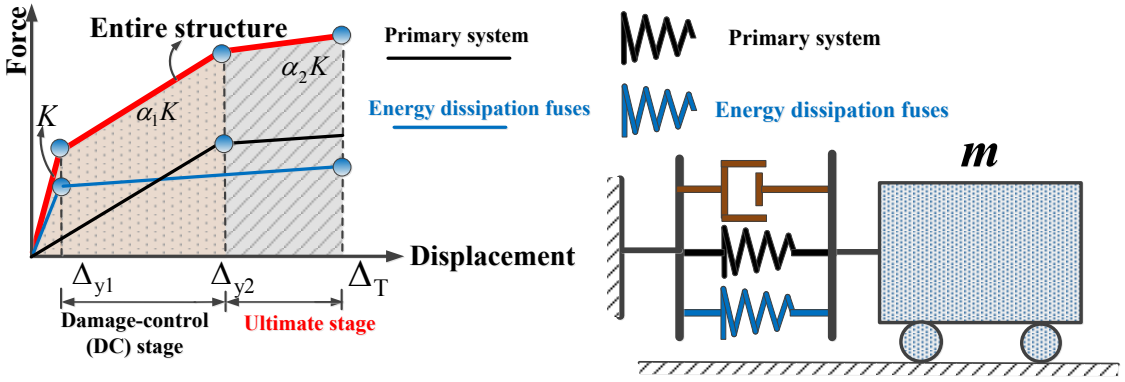

(a) (b)

Fig. 1 Damage-control structures with energy dissipation fuses: (a) typical pushover curve and (b) SDOF analogy.

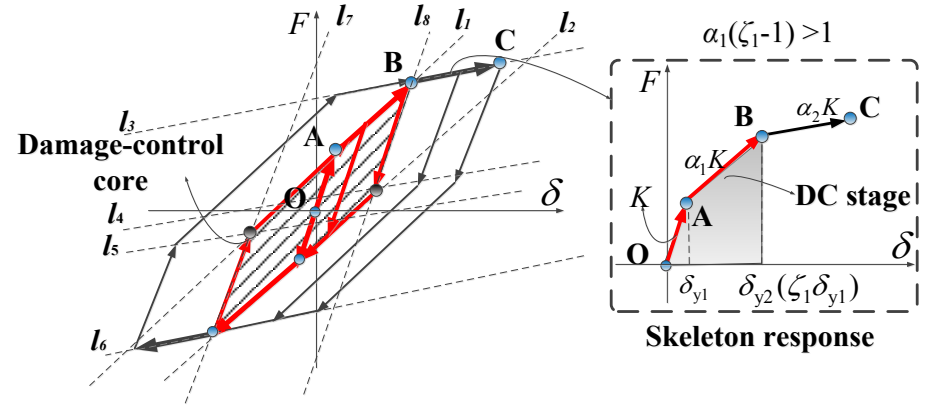

(a)

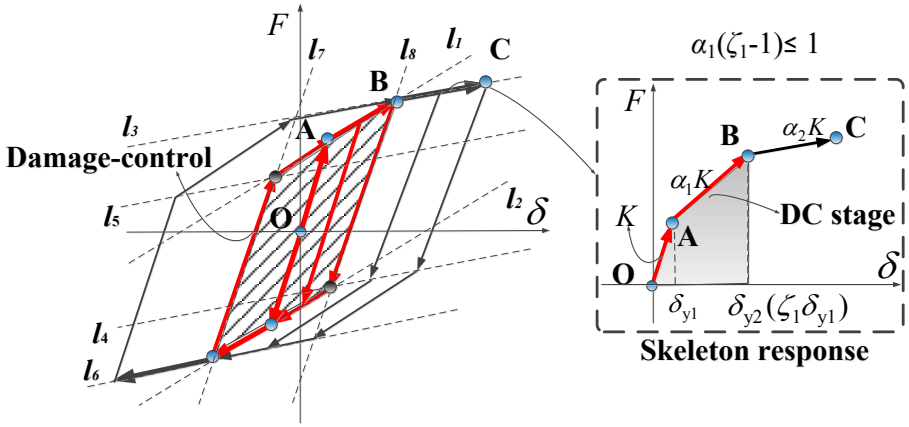

(b)

Fig. 2 Hysteretic model of the SDOF system representing a damage-control structure with energy dissipation fuses in the ultimate stage: (a) $\alpha_1(\zeta_1-1)>1$ and (b) $\alpha_1(\zeta_1-1)\leq 1$.

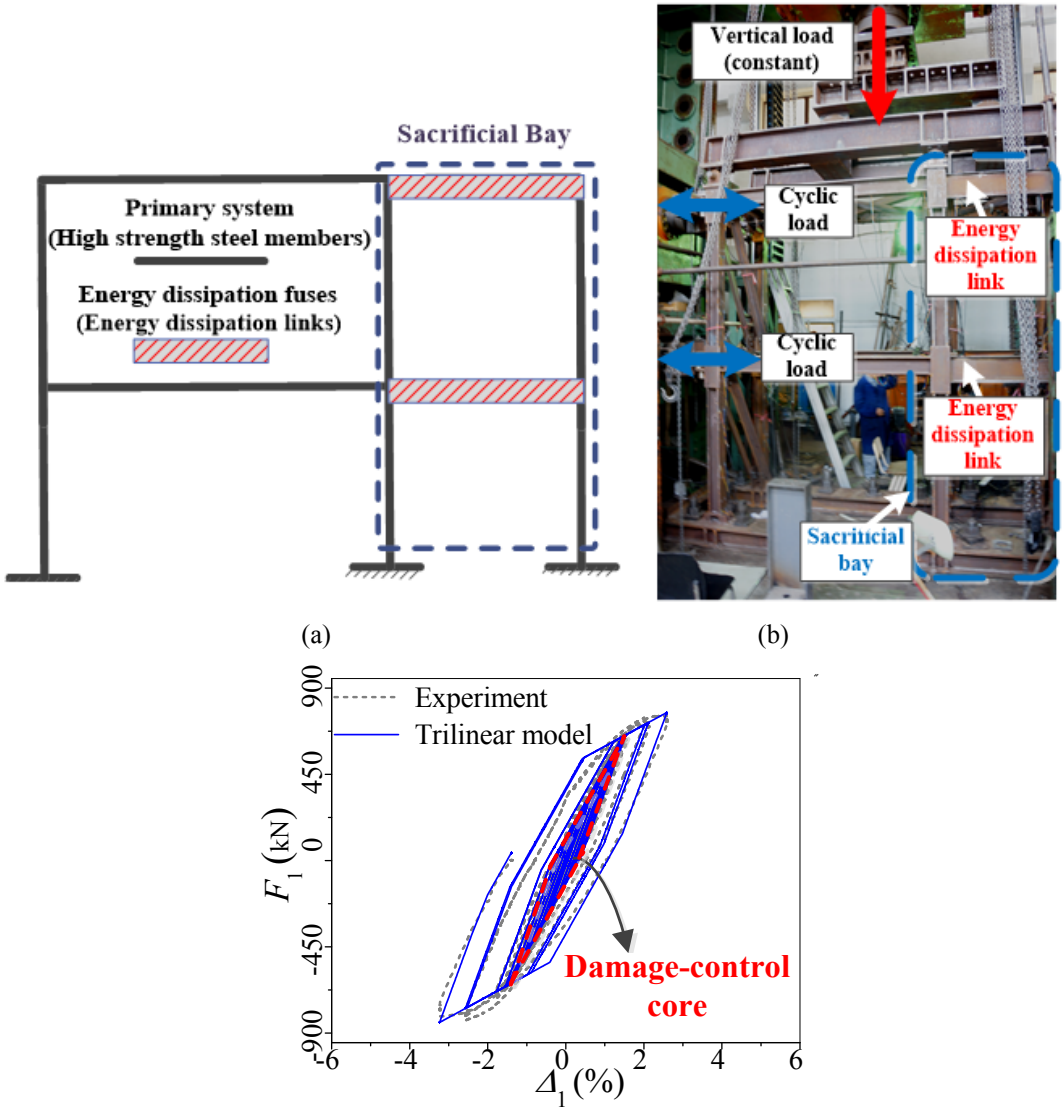

(c)

Fig. 3 Validation of the trilinear hysteretic model: (a) design concept of a typical damage-control structure with energy dissipation fuses, (b) test setup and (c) comparison of test result and the trilinear model.

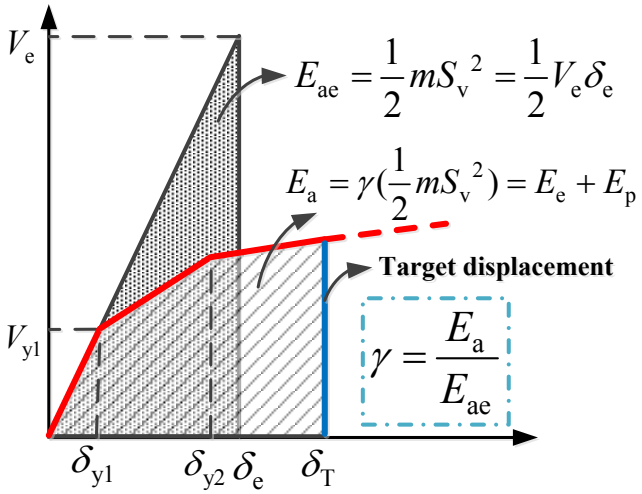

Fig. 4 Energy factor of a trilinear SDOF system with presence of the DC stage.

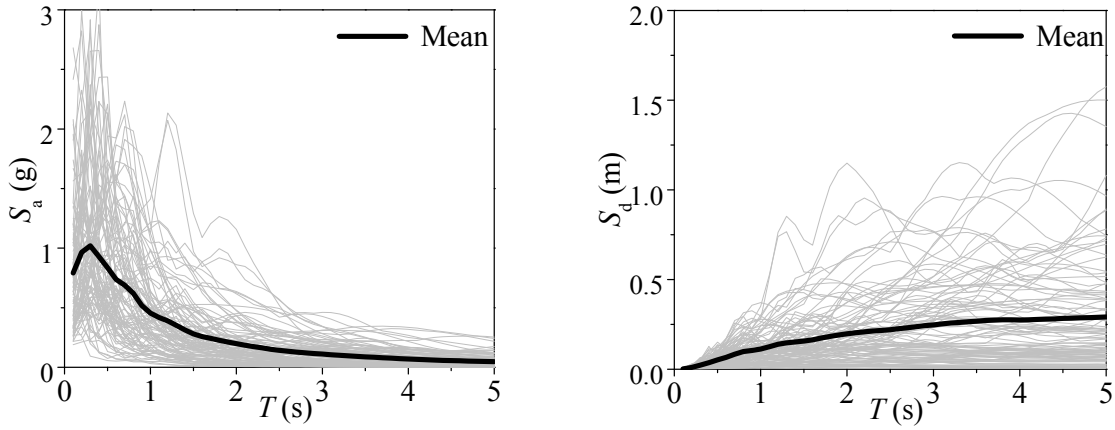

(a) (b)

Fig. 5 Ground motions spectra: (a) pseudo acceleration spectra and (b) displacement spectra [5, 9].

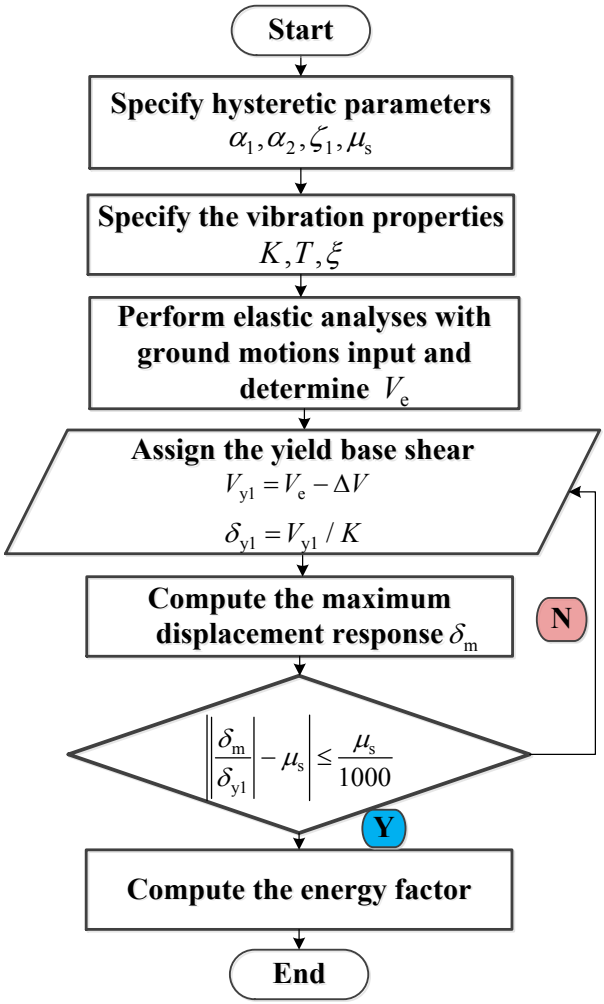

Fig. 6 Flowchart of analysis procedure.

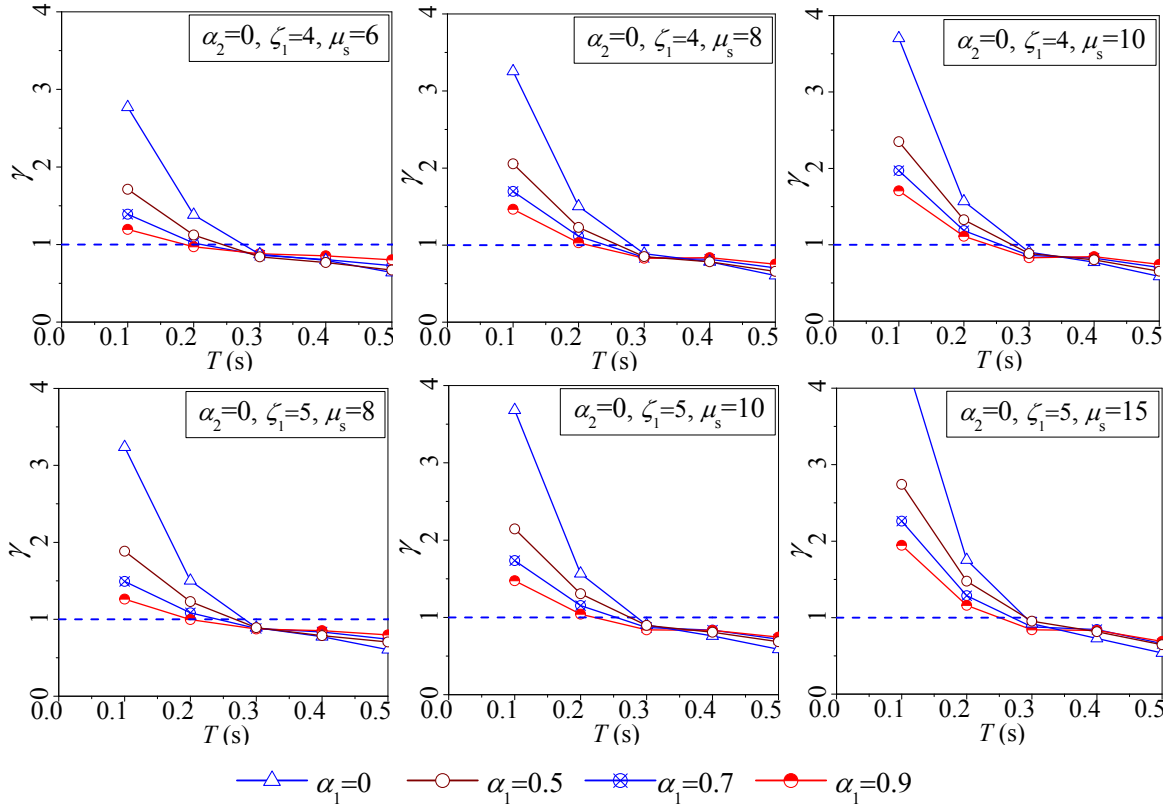

(a)

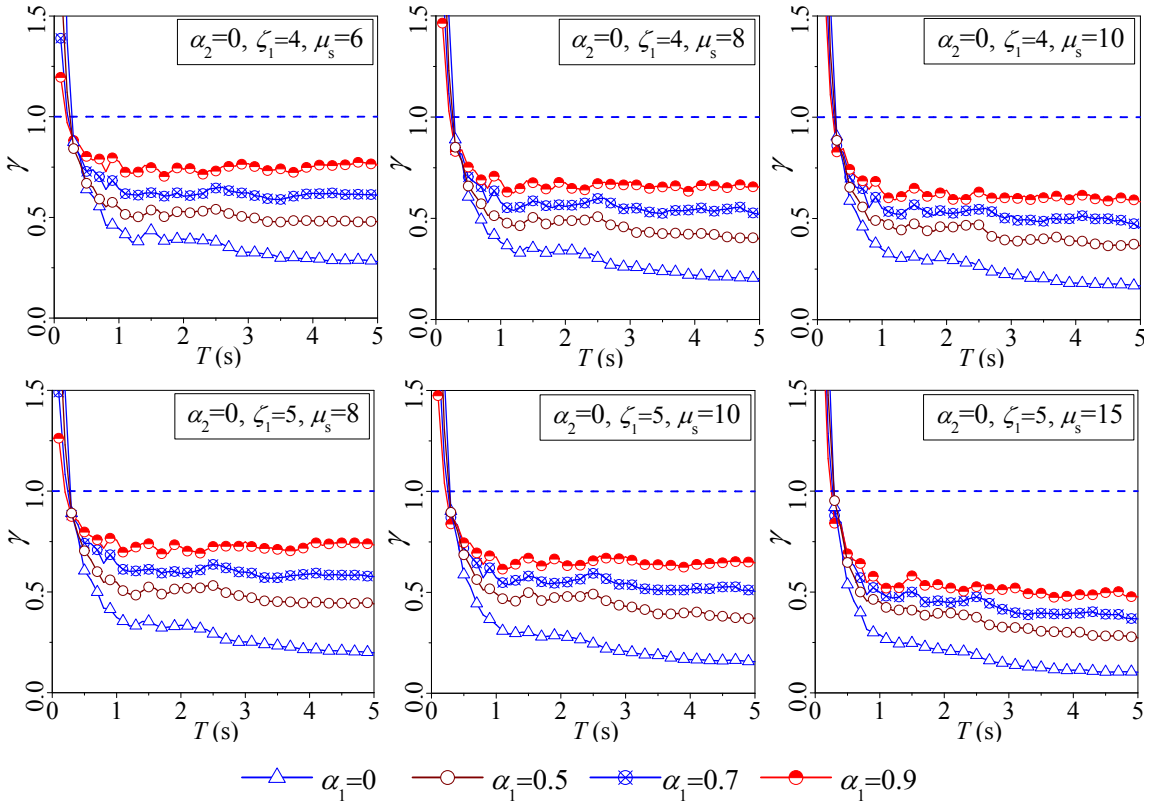

(b)

Fig. 7 Effect of post-yielding stiffness ratio (α_1) in the DC stage and the inelastic deformation levels (ζ_1 and μ_s): (a) T<0.5 s and (b) T<5 s.

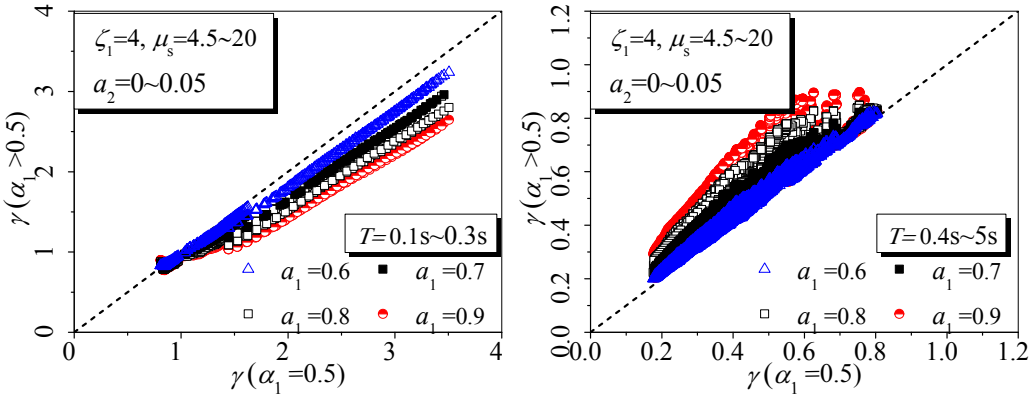

Fig. 8 Effect of the post-yielding stiffness ratio (α_1) in the DC stage.

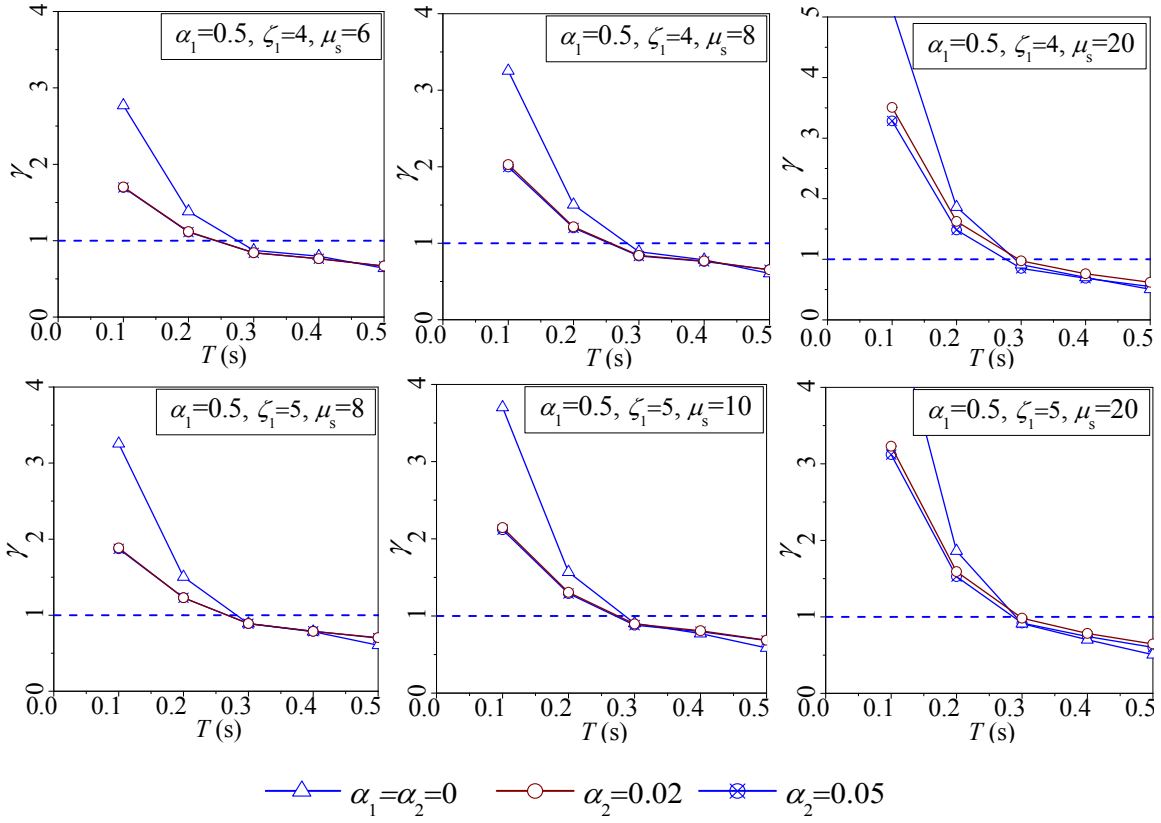

(a)

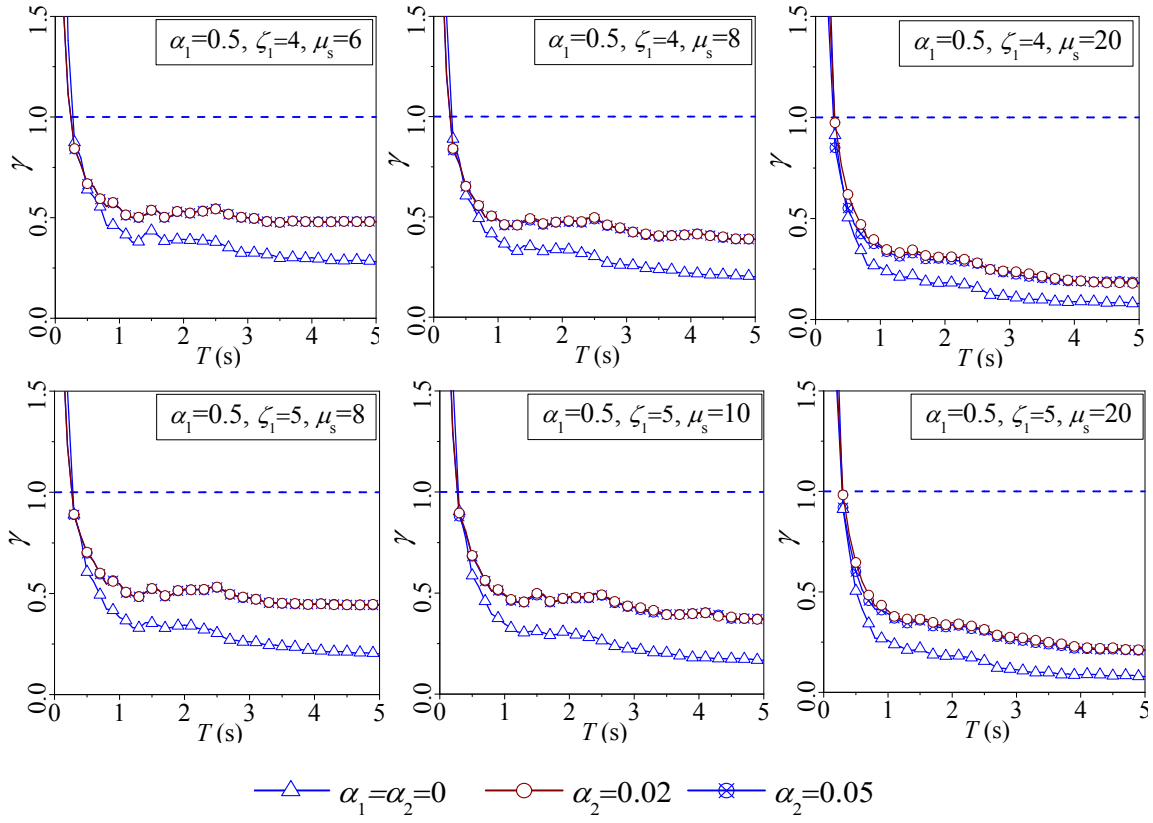

(b)

Fig. 9 Effect of post-yielding stiffness ratio (α_2) in the ultimate stage and the inelastic deformation levels (ζ_1 and μ_s): (a) T<0.5 s and (b) T<5 s.

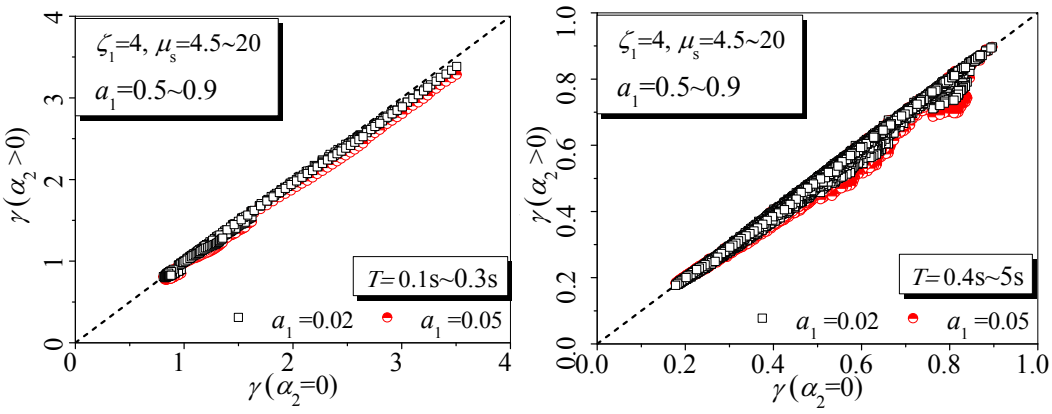

Fig. 10 Effect of the post-yielding stiffness ratio (α_2) in the ultimate stage.

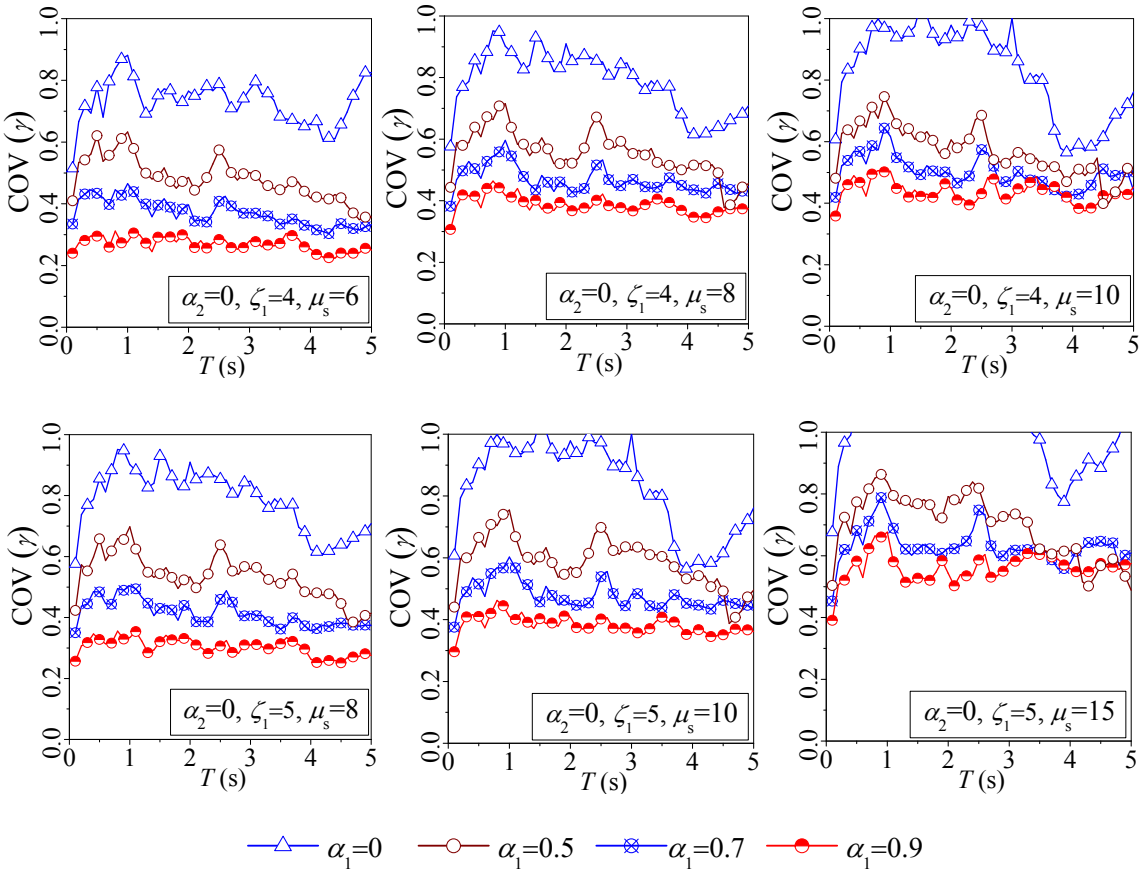

(a)

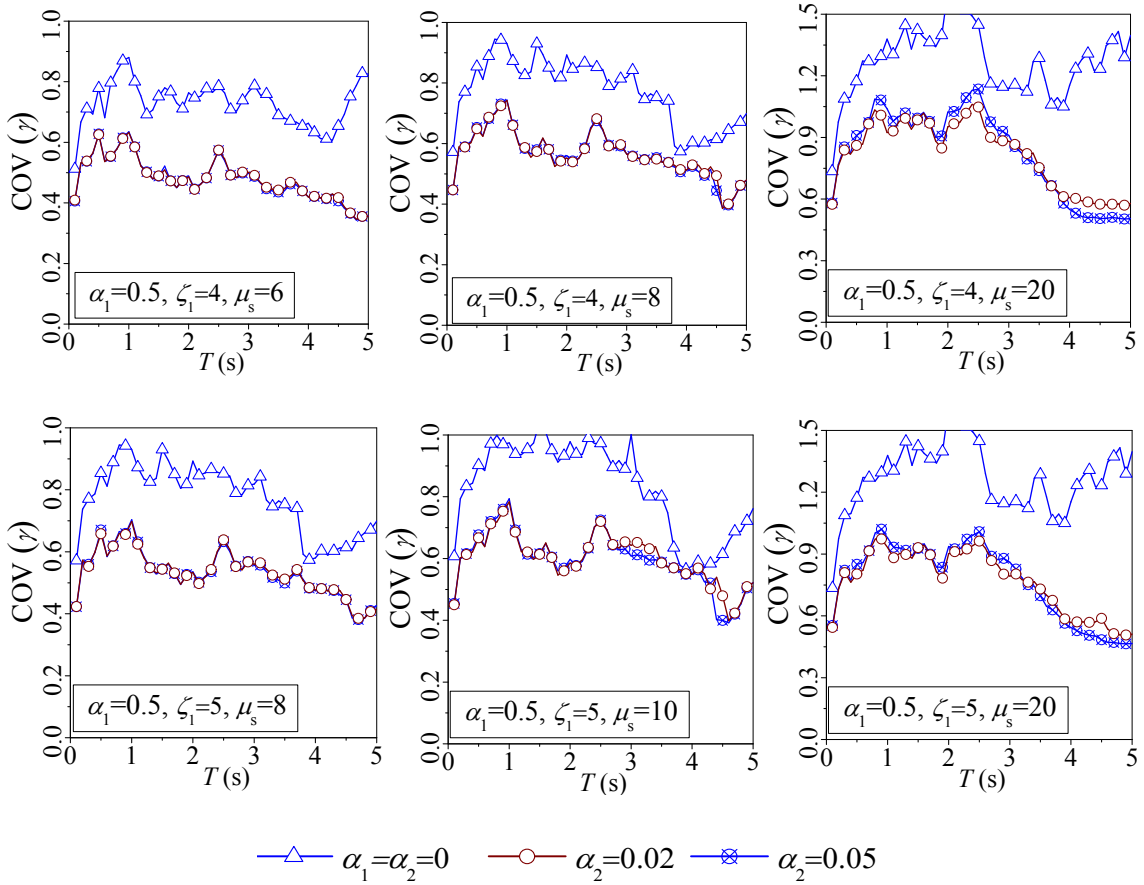

(b)

Fig. 11 Representative COV spectra of mean energy factor: (a) EP SDOF systems and trilinear SDOF systems (α_2=0) and (b) EP SDOF systems and trilinear SDOF systems (α_1=0.5).

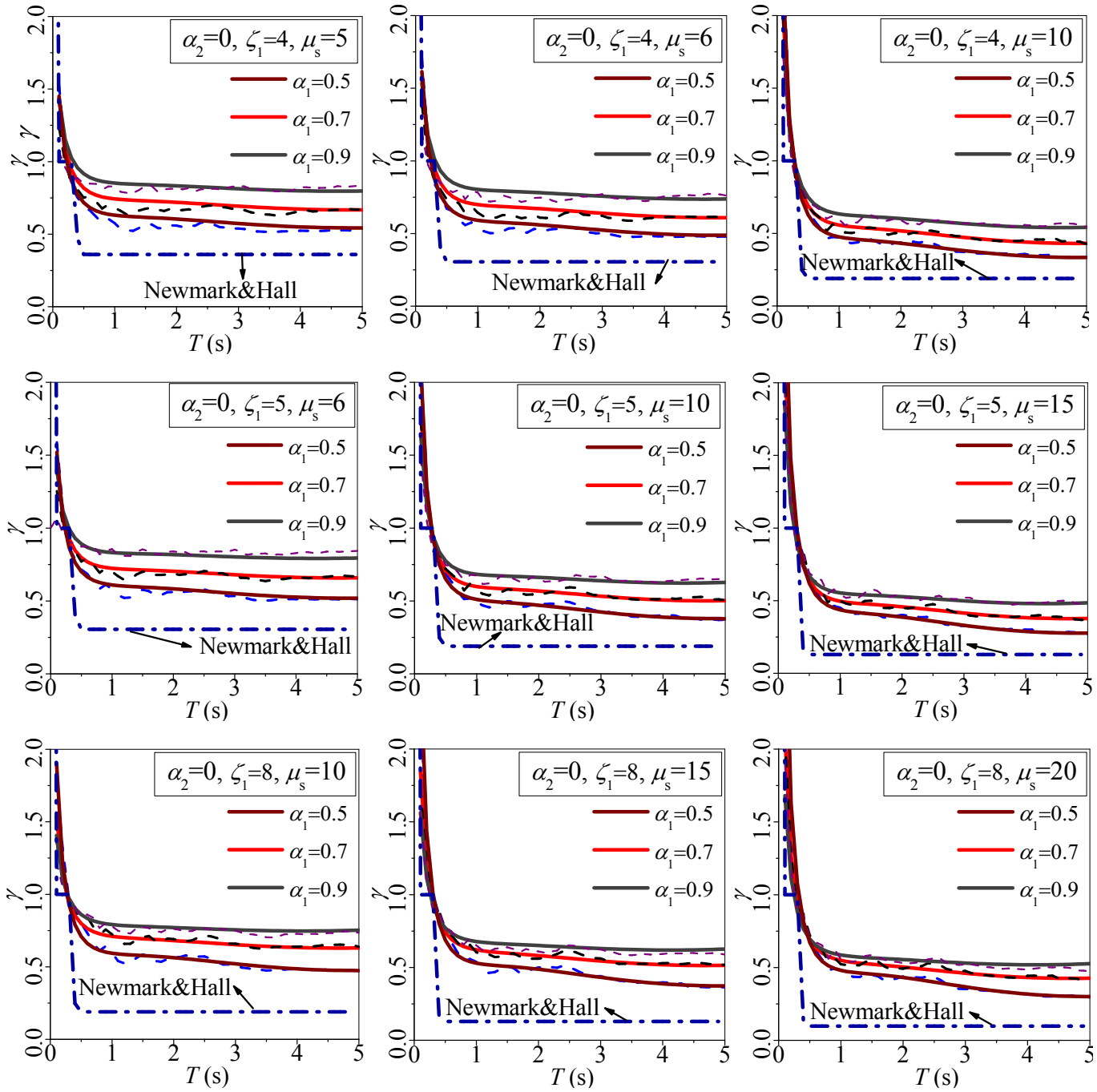

Fig. 12 Representative energy factor spectra determined by inelastic spectral analyses and empirical expressions.

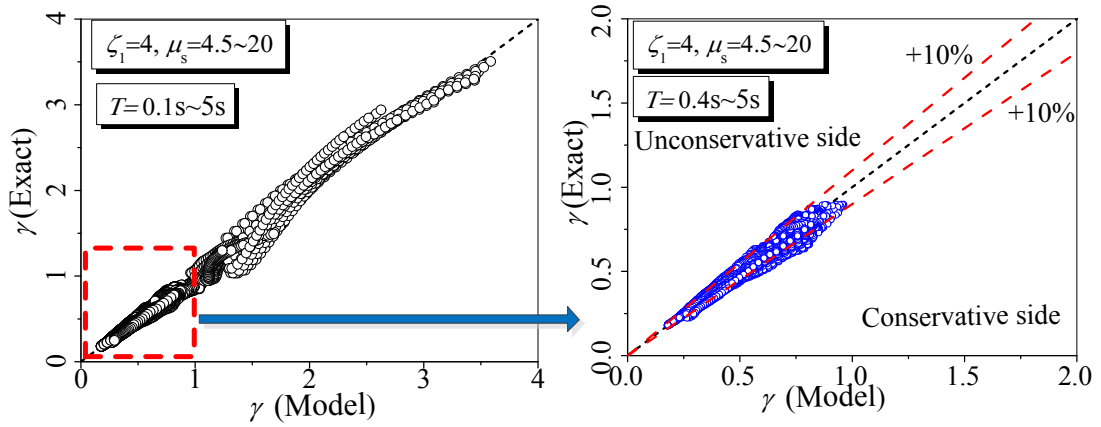

(a)

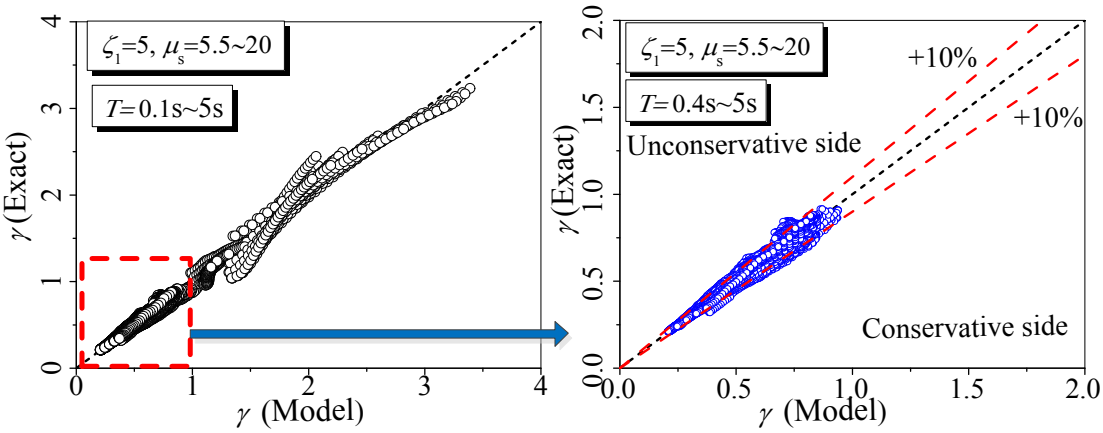

(b)

Fig. 13 Data points comparison of representative cases: (a) ζ_1=4 and (b) ζ_1=5.

Table 1 Regressed coefficients a_i, b_i, c_i, d_i, f_i (i=1~6) for the proposed empirical expressions

Deformation range of the DC stage	Coefficient	a_i, b_i, c_i, d_i, f_i (i=1~6)						R^2
		i=1	i=2	i=3	i=4	i=5	i=6	
Case ζ_1=4	a_i	0.2298	-0.2883	-0.6813	0.1134	3.5968	0.3253	0.979
	b_i	0.0699	-0.0977	-0.1256	0.0444	0.4968	0.0843	
	c_i	0.5000	0.0200	-0.1609	-0.3567	0.4747	0.7490	
	d_i	-0.7183	0.9598	1.5820	-0.4014	-5.3682	-1.2210	
	f_i	0.8957	0.8269	0.1496	0.6087	-0.0630	-11.3600	
Case ζ_1=5	a_i	0.2313	-0.3427	-0.5885	0.1508	1.7069	0.4270	0.994
	b_i	0.0662	-0.1016	-0.1026	0.0481	0.2285	0.0903	
	c_i	-0.3482	0.5280	0.5721	-0.2394	-0.5598	-0.5587	
	d_i	-0.7004	1.0604	1.2097	-0.4767	-1.4835	-1.1954	
	f_i	0.7913	0.2446	1.0373	-0.1375	-11.2200	0.1233	
Case ζ_1=6	a_i	0.2174	-0.3385	-0.0366	0.1528	2.7041	-0.4758	0.989
	b_i	0.0625	-0.1015	0.0210	0.0496	0.1989	-0.0963	
	c_i	-0.3289	0.5279	-0.1783	-0.2478	-2.3235	0.6926	
	d_i	-0.6874	1.1344	-0.4102	-0.5426	-3.5225	1.4080	
	f_i	0.9546	-0.2091	-0.7595	0.1488	-21.5330	4.2726	
Case ζ_1=7	a_i	0.2338	-0.4087	-0.2552	0.1986	-1.1221	0.1897	0.995
	b_i	0.0655	-0.1178	-0.0476	0.0608	-0.2493	0.0664	
	c_i	-0.3509	0.6283	0.2782	-0.3150	0.2764	-0.3408	
	d_i	-0.7432	1.3658	0.5575	-0.6973	0.9458	-0.7301	
	f_i	0.8614	0.0678	1.2263	-0.0165	-5.1660	-0.3468	
Case ζ_1=8	a_i	0.2462	-0.4714	-0.1512	0.2488	6.6772	-0.2081	0.982
	b_i	0.0659	-0.1273	-0.0274	0.0695	1.1544	-0.0100	
	c_i	-0.3608	0.6987	0.0861	-0.3758	-7.5071	0.2214	
	d_i	-0.7740	1.5349	0.2628	-0.8348	-13.5803	0.2400	
	f_i	0.7985	0.3304	-0.6053	-0.2567	-60.2938	4.4554	